Supporting Information: Modeling the Relationship between the p53 C-terminal Domain and its Binding Partners Using Molecular Dynamics

William J. Allen, [1] *Daniel G. S. Capelluto,* [2] *Carla V. Finkielstein,* [3] *and David R. Bevan** [1]

[1] Department of Biochemistry, Virginia Polytechnic Institute and State University, 111 Engel Hall (0308), Virginia Tech, Blacksburg, VA 24061

[2] Protein Signaling Domains Laboratory, Department of Biological Sciences, Virginia Polytechnic Institute and State University, 1981 Kraft Dr. (0913), Virginia Tech, Blacksburg, VA 24061

[3] Integrated Cellular Responses Laboratory, Department of Biological Sciences, Virginia Polytechnic Institute and State University, 1981 Kraft Dr. (0913), Virginia Tech, Blacksburg, VA 24061

* Corresponding author: E-mail - drbevan@vt.edu; Phone - (540) 231-5040; Fax - (540) 231-9070.

Modified Lysine Parameters

Listed below are the parameters for acetylated lysine (Table S1), methylated lysine (Table S2), and the original lysine parameters from ffG53a6.rtp (Table S3). The numbers in the first column correspond to atom numbers as shown in Figure S1.

Table S1. Acetylated lysine parameters.

Atom Number	Atom Type	Charge Group Number	Charge
1	N	1	-0.31
2	H	1	0.31
3	CH1	2	0
4	CH2	2	0
5	CH2	3	0
6	CH2	3	0
7	CH2	3	0
8	N	4	-0.31
9	H	4	0.31
10	C	5	0.45
11	O	5	-0.45
12	CH3	6	0
13	C	7	0.45
14	O	7	-0.45

Table S2. Methylated lysine parameters.

Atom Number	Atom Type	Charge Group Number	Charge
1	N	1	-0.31
2	H	1	0.31
3	CH1	2	0
4	CH2	2	0
5	CH2	3	0
6	CH2	3	0
7	CH2	4	0.127
8	NL	4	0.129
9	H	4	0.3085
10	H	4	0.3085
11	CH3	4	0.127
12	C	5	0.45
13	O	5	-0.45

Table S3. Original lysine parameters from ffG53a6.rtp (listed as [LYSH]).

Atom Number	Atom Type	Charge Group Number	Charge
1	N	1	-0.31
2	H	1	0.31
3	CH1	2	0
4	CH2	2	0
5	CH2	3	0
6	CH2	3	0
7	CH2	4	0.127
8	NL	4	0.129
9	H	4	0.248
10	H	4	0.248
11	H	4	0.248
12	C	5	0.45
13	O	5	-0.45

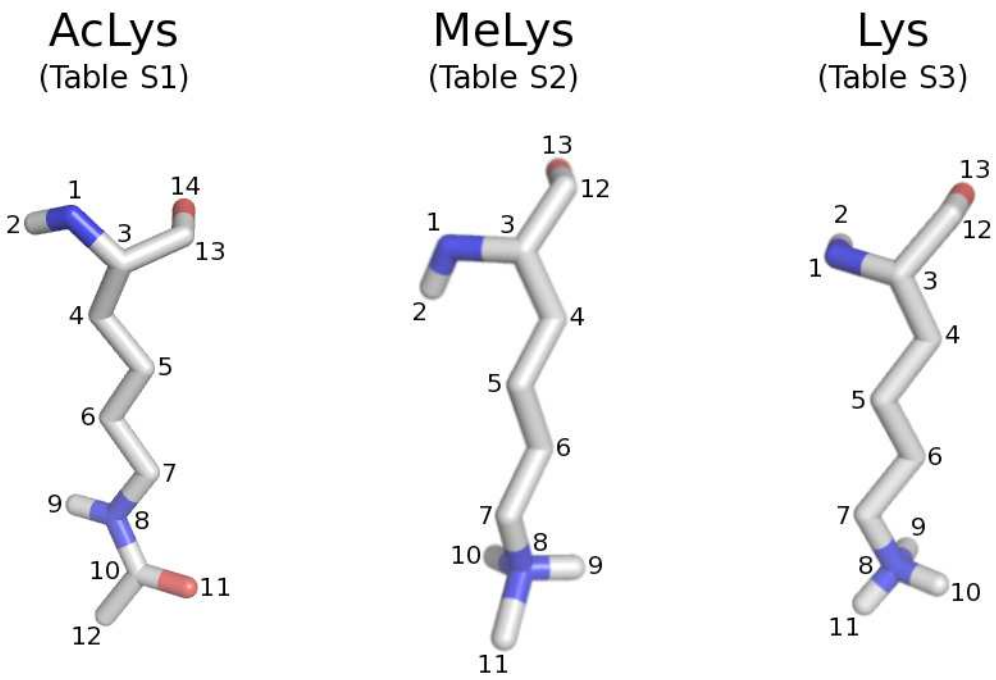

Figure S1. Atom numbering scheme for acetylated lysine (AcLys), methylated lysine (MeLys), and unmodified lysine (Lys).

NMR Structure Ensemble Comparison

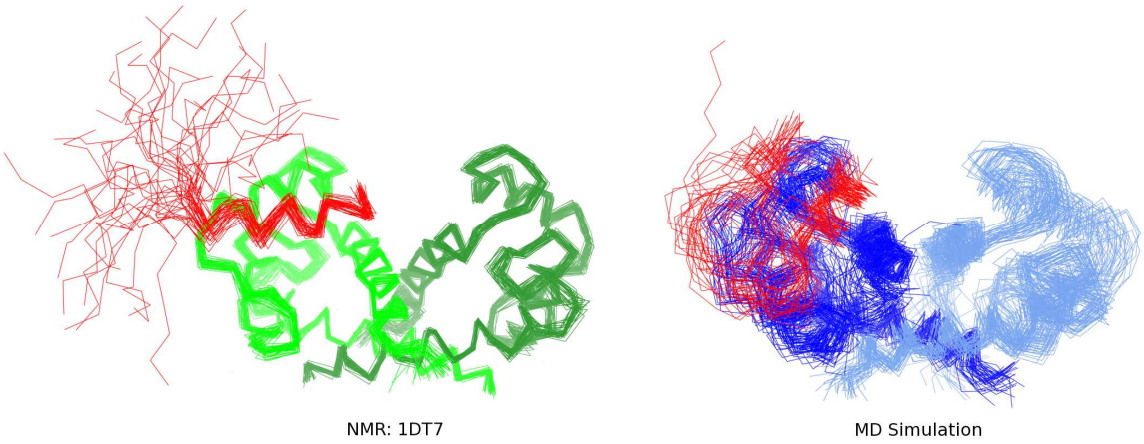

Figure S2. (Left) Overlay of forty 1DT7 NMR structures. S100B(ββ) subunits are shown in green and forest green, the p53 CTD is shown in red. (Right) Overlay of forty 1DT7 structures from evenly spaced intervals along the 100 ns MD trajectory. S100B(ββ) subunits are shown in dark blue and light blue, the p53 CTD is shown in red.

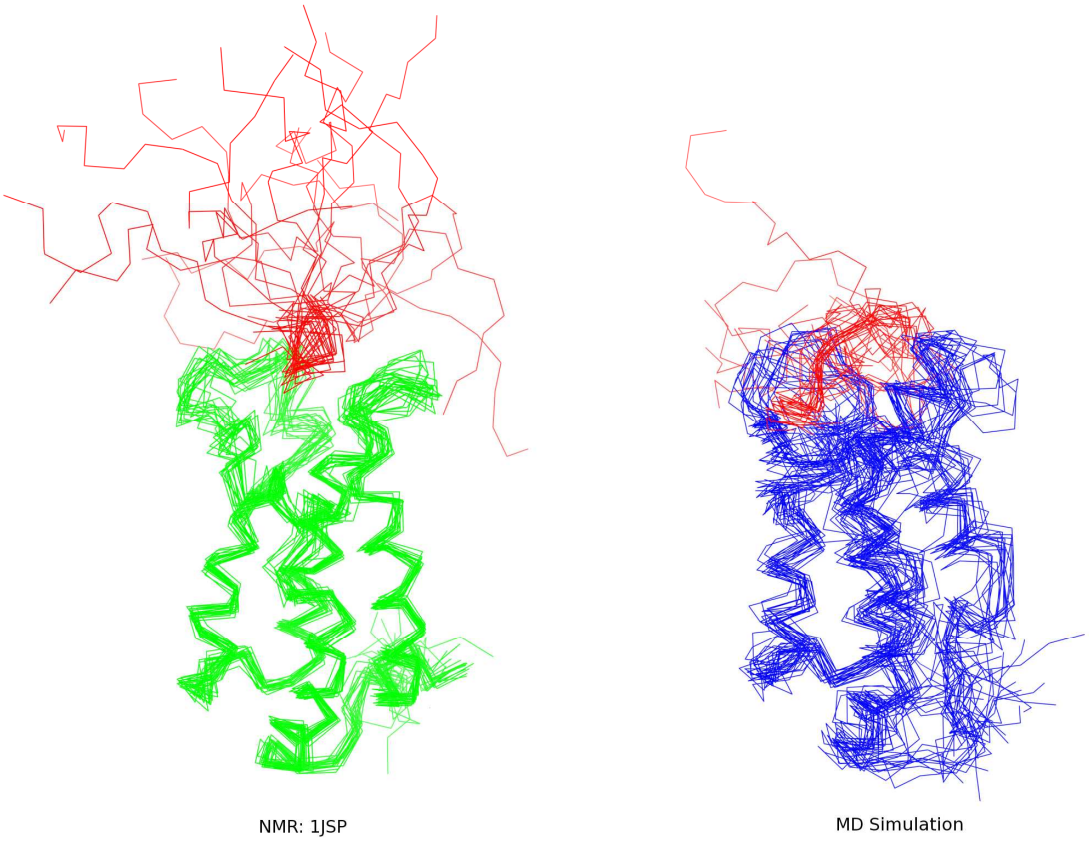

Figure S3. (Left) Overlay of twenty 1JSP NMR structures. The CBP bromodomain is shown in green and the p53 CTD is shown in red. (Right) Overlay of twenty 1JSP structures from evenly spaced intervals along the 100 ns MD trajectory. The CBP bromodomain is shown in blue and the p53 CTD is shown in red.

Table S4. Radius of gyration (R_g). Values are in nm.

		NMR	MD
1DT7	S100B(ββ)	1.70±0.01	1.74±0.02
	p53 CTD	1.14±0.10	0.91±0.02
1JSP	CBP bromodomain	1.47±0.01	1.53±0.02
	p53 CTD	1.24±0.10	1.19±0.12

Table S5. Secondary structure content. Values are in number of residues.

			Coil	α-Helix	β-Sheet	Bend	Turn
1DT7	S100B(ββ)	NMR	21.3±0.3	112.6±0.5	11.8±0.1	20.7±0.6	16.4±0.8
		MD	36.8±3.2	102.1±2.7	3.0±2.8	30.7±3.8	7.6±3.8
	p53 CTD	NMR	8.1±1.3	7.3±0.6	-	1.7±1.3	3.6±0.8
		MD	10.5±1.2	7.0±1.0	-	4.9±1.6	0.5±1.0
1JSP	CBP bromodomain	NMR	21.5±3.4	51.9±3.4	-	24.0±3.6	20.5±4.3
		MD	35.5±3.7	53.7±3.4	-	15.4±4.0	13.9±4.4
	p53 CTD	NMR	16.7±2.2	-	-	2.6±1.4	0.8±1.6
		MD	13.6±2.0	-	-	3.5±2.0	2.0±1.5

Supplemental Figures for 1H26

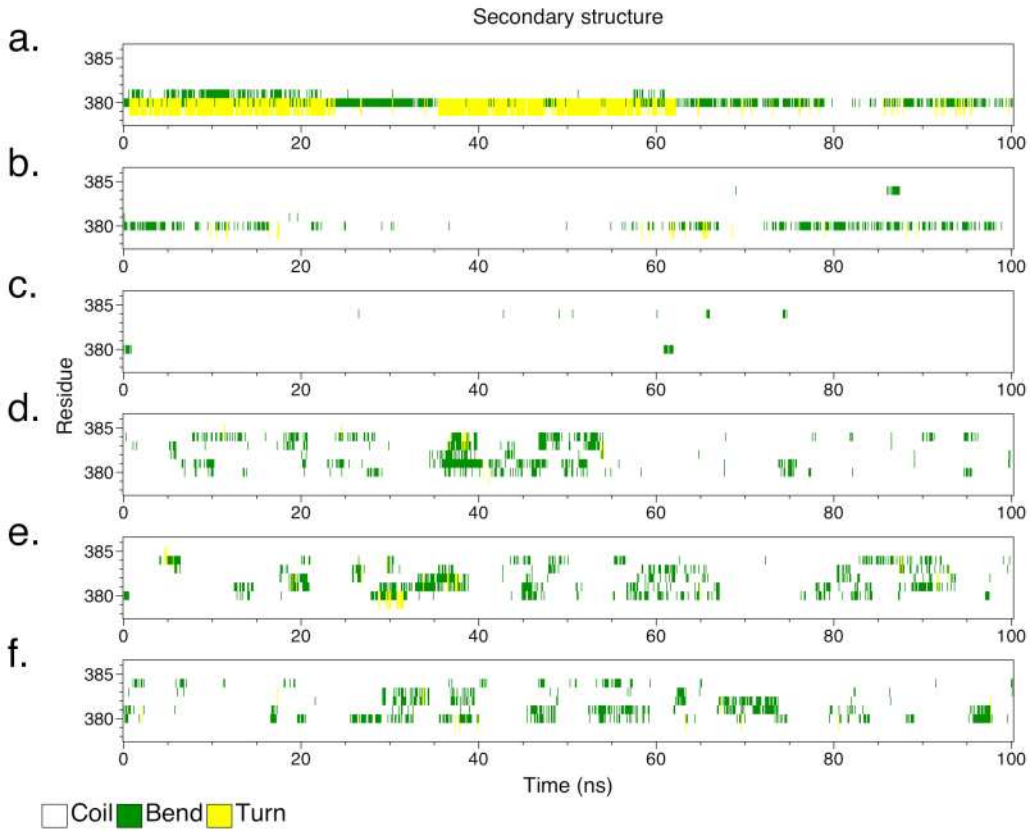

Figure S4. DSSP analysis for 1H26. Panels **(a–c)** show the secondary structure content of the p53 CTD when bound to cyclin A. Panels **(d–f)** show the secondary structure content of the unbound p53 CTD.

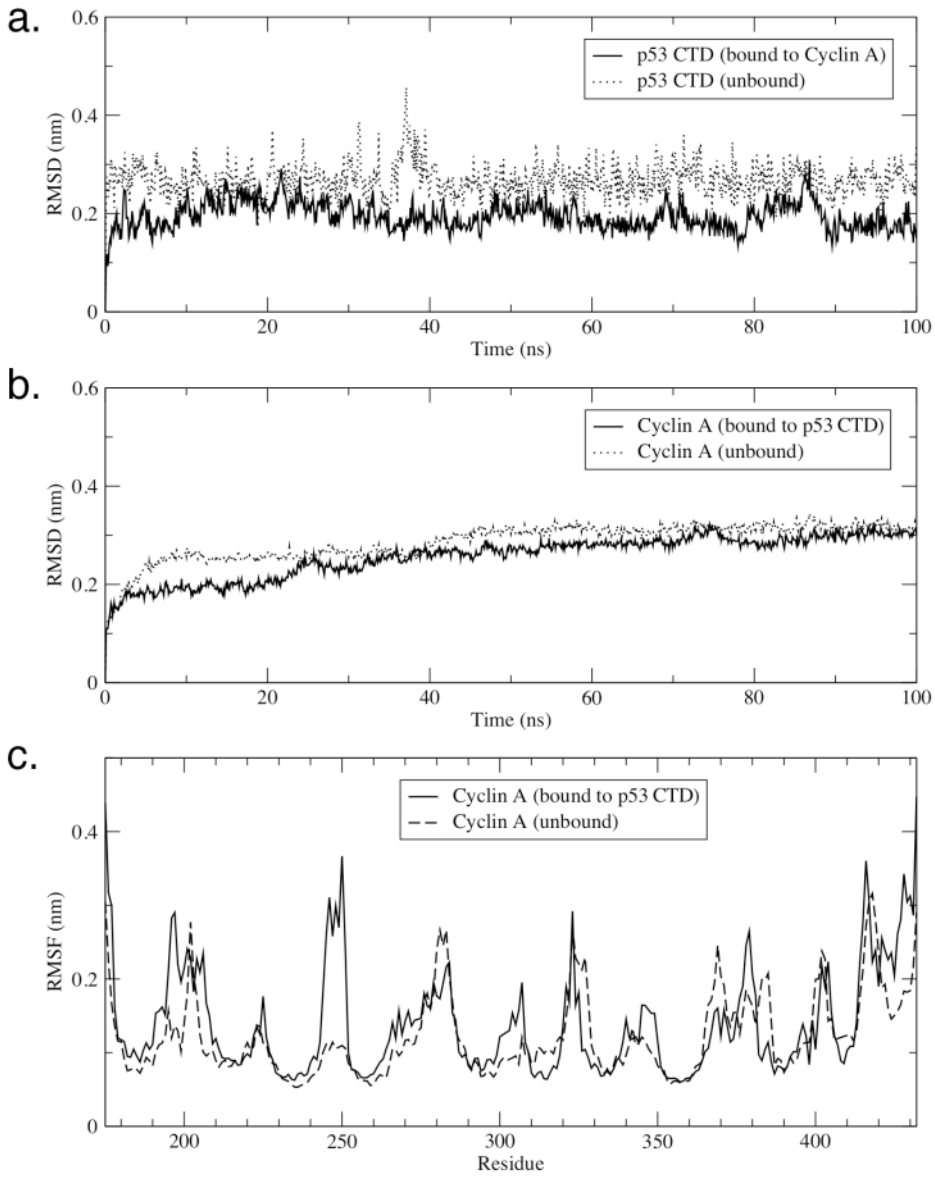

Figure S5. RMSD and RMSF analysis for 1H26. Panel **(a)** shows the average backbone RMSD for the three replicates of the p53 CTD in complex with cyclin A (solid line), and in the absence of cyclin A (dotted line). Panel **(b)** shows the average backbone RMSD for the three replicates of the cyclin A receptor in complex with the p53 CTD (solid line) and in the absence of the p53 CTD (dotted line). Panel **(c)** represents the RMSF of cyclin A in complex with the p53 CTD (solid line), and in the absence of the p53 CTD (dashed line).

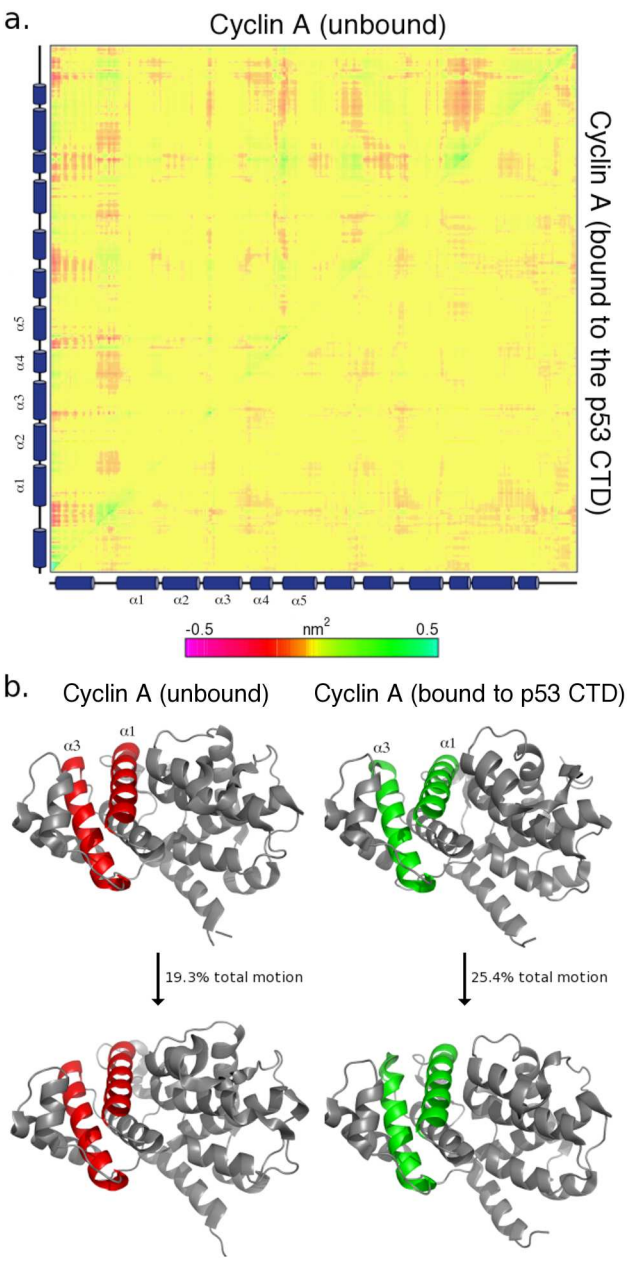

Figure S6. PC analysis for 1H26. Panel **(a)** shows a covariance matrix illustrating correlated and anti-correlated motions within cyclin A in the absence of the p53 CTD (top left) and when bound to the p53 CTD (bottom right). The secondary structure of the cyclin A backbone is represented along the axes (from left-to-right, and from bottom-to-top). Panel **(b)** shows the motion of the largest eigenvector on the cyclin A structure in

the absence of the p53 CTD (left) and when bound to the p53 CTD (right). The sites on cyclin A that bind the p53 CTD are colored red and green.

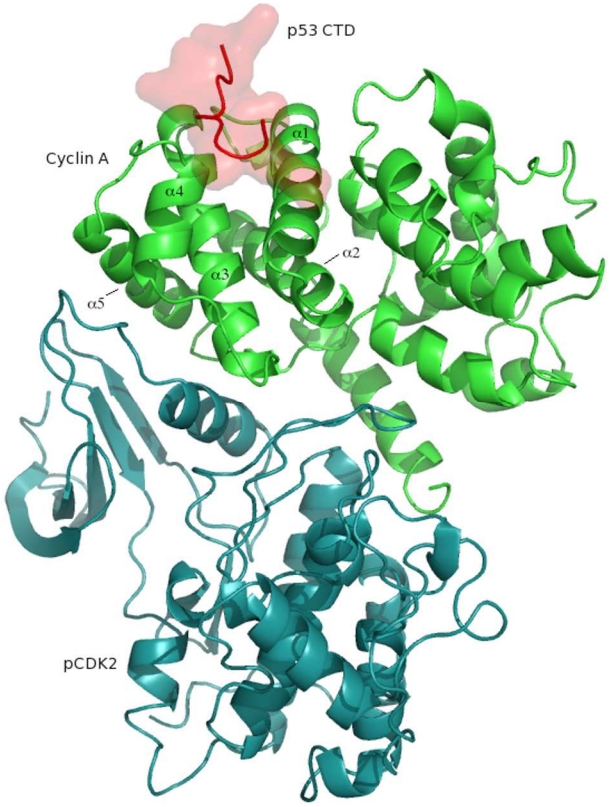

Figure S7. Surface rendering and cartoon of the p53 CTD (colored in red). Cyclin A is shown in green cartoon, whereas pCDK2 is shown in blue cartoon. The five helices that form the p53 CTD binding site (α1-α5) in cyclin A are labeled.

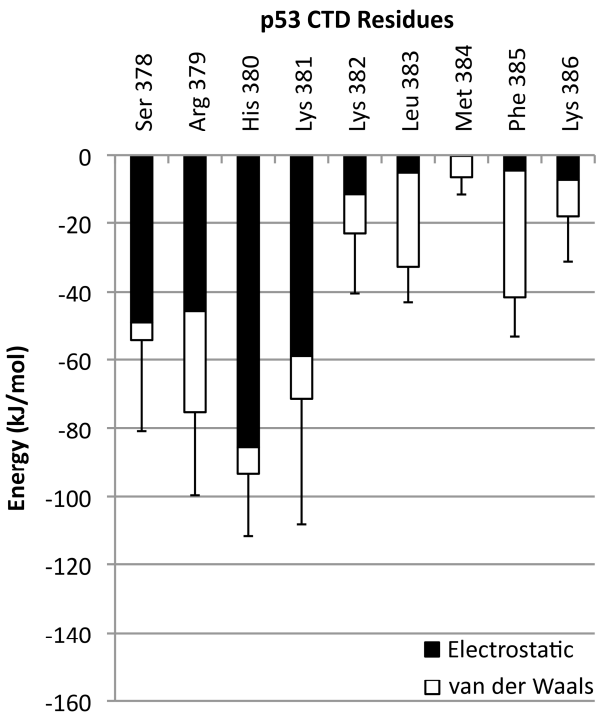

Figure S8. Potential energy of interaction between the p53 CTD and cyclin A by residue. The electrostatic contribution is shown in black, and the van der Waals contribution is shown in white. Error bars represent the standard deviation in the sum of the interactions.

Supplemental Figures for 1JSP

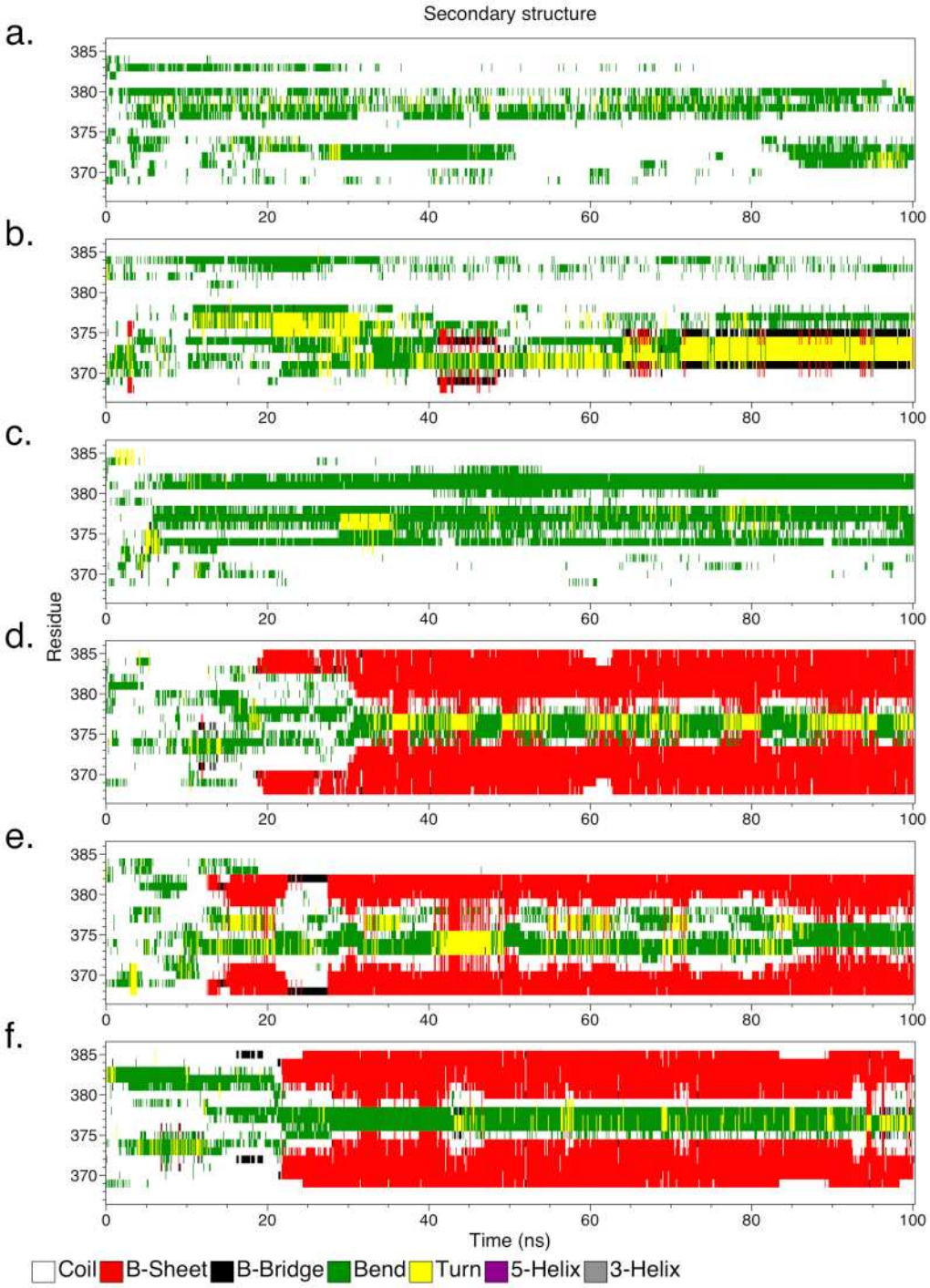

Figure S9. DSSP analysis for 1JSP. Panels **(a–c)** show the secondary structure content of the p53 CTD when bound to the CBP bromodomain. Panels **(d–f)** show the secondary structure content of the unbound p53 CTD.

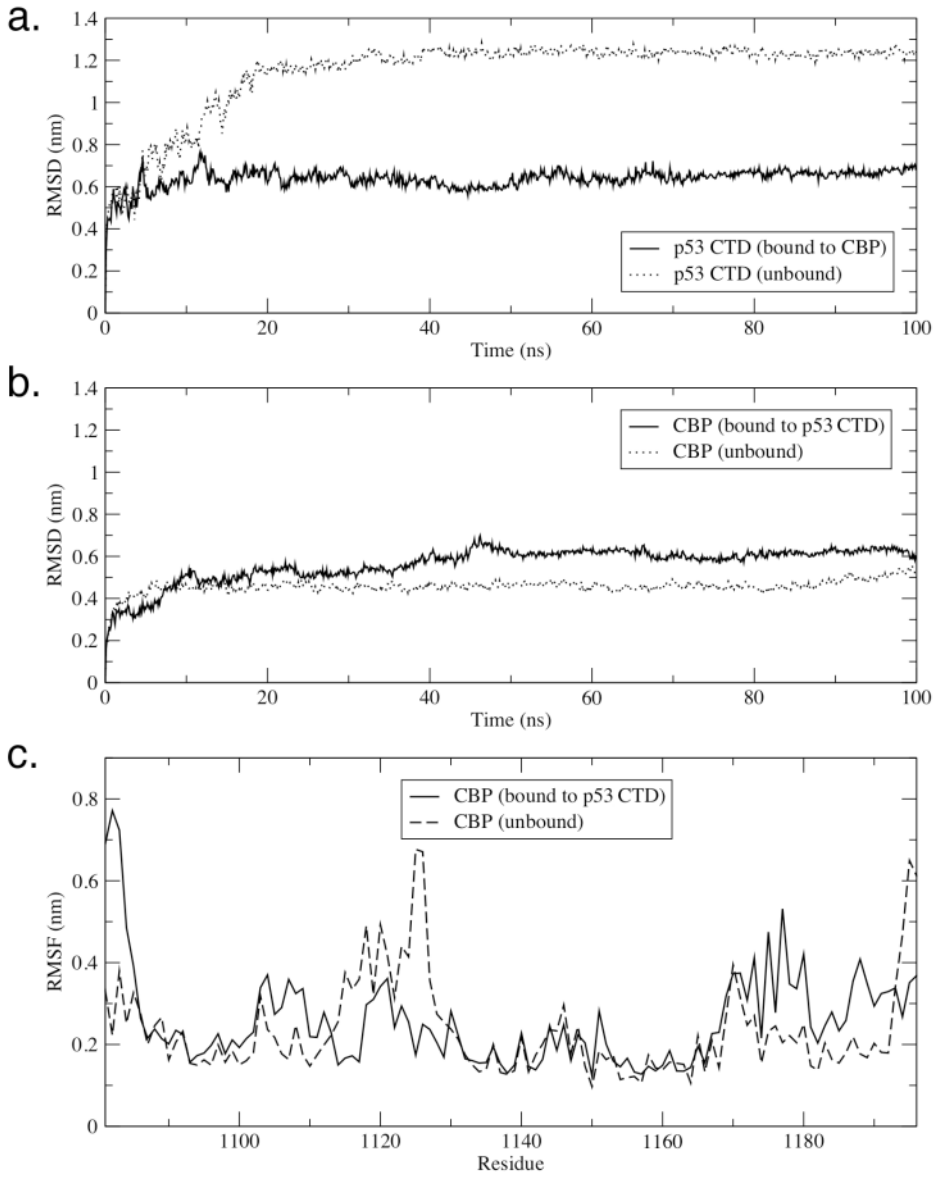

Figure S10. RMSD and RMSF analysis for 1JSP. Panel **(a)** shows the average backbone RMSD for the three replicates of the p53 CTD in complex with the CBP bromodomain (solid line), and in the absence of the CBP bromodomain (dotted line). Panel **(b)** shows the average backbone RMSD for the three replicates of the CBP bromodomain receptor in complex with the p53 CTD (solid line) and in the absence of the p53 CTD (dotted line). Panel **(c)** represents of the RMSF of the CBP bromodomain in complex with the p53 CTD (solid line), and in the absence of the p53 CTD (dashed line).

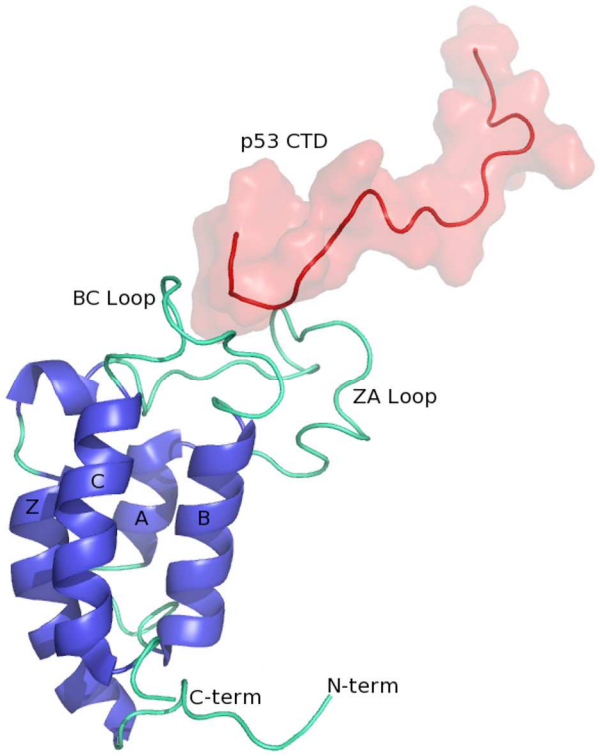

Figure S11. Surface rendering and cartoon of the p53 CTD (shown in red). The CBP bromodomain is shown in cartoon. α-Helices are colored dark blue, and loops are colored light blue.

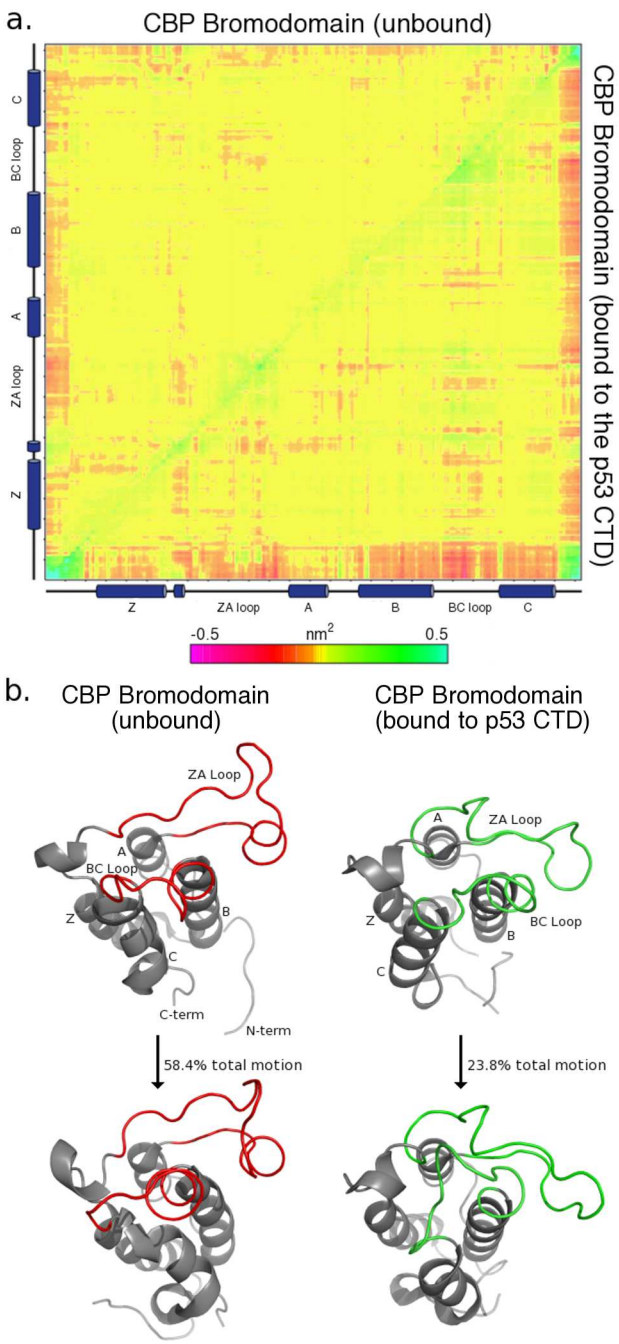

Figure S12. PC analysis for 1JSP. Panel **(a)** shows a covariance matrix illustrating correlated and anti-correlated motions within the CBP bromodomain in the absence of the p53 CTD (top left) and when bound to the p53 CTD (bottom right). The secondary structure of the CBP bromodomain backbone is represented along the axes (from left-to-right, and from bottom-to-top). Panel **(b)** shows the motion of the

largest eigenvector on the CBP bromodomain structure in the absence of the p53 CTD (left) and when bound to the p53 CTD (right). The sites on the CBP bromodomain that bind the p53 CTD are colored red and green.

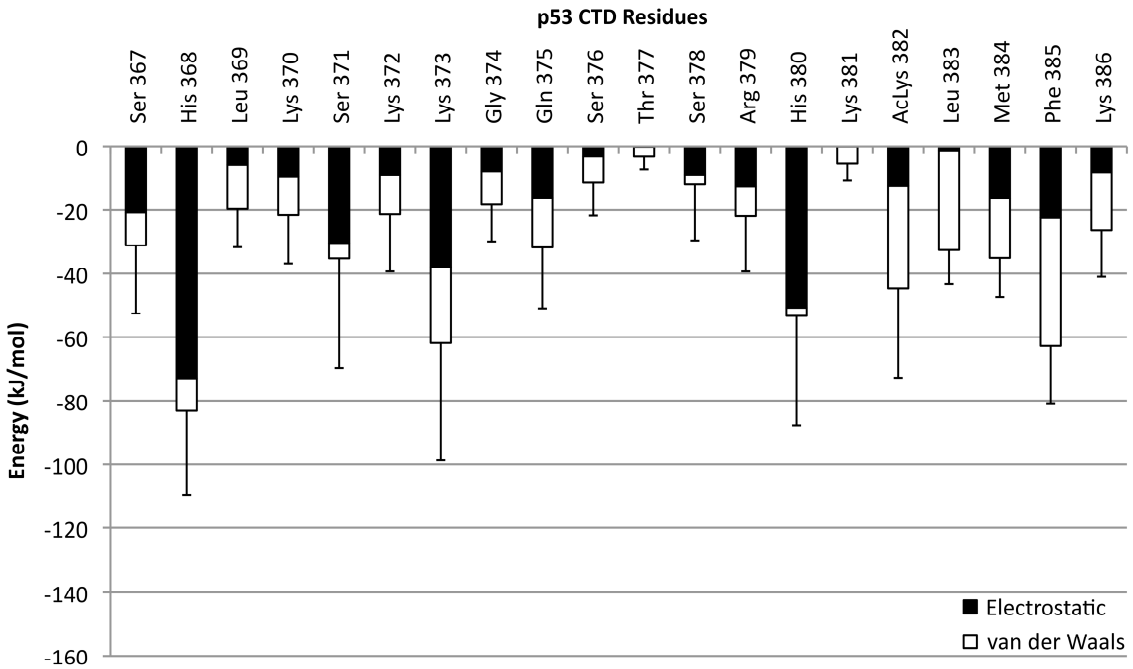

Figure S13. Potential energy of interaction between the p53 CTD and the CBP bromodomain by residue. The electrostatic contribution is shown in black, and the van der Waals contribution is shown in white. Error bars represent the standard deviation in the sum of the interactions.

Supplemental Figures for 1XQH

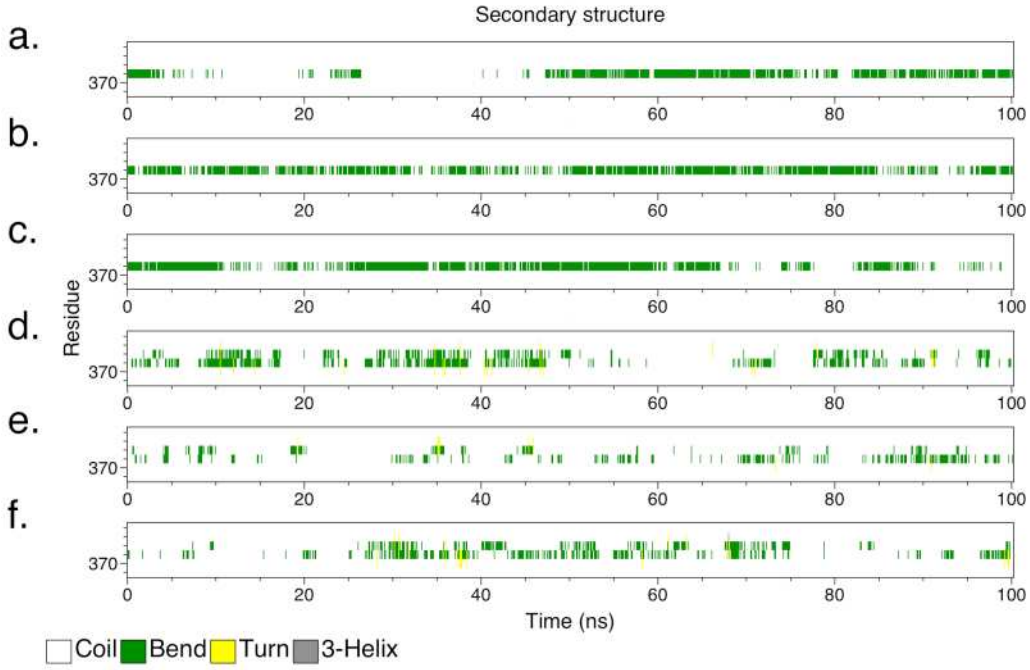

Figure S14. DSSP analysis for 1XQH. Panels **(a–c)** show the secondary structure content of the p53 CTD when bound to Set9. Panels **(d–f)** show the secondary structure content of the unbound p53 CTD.

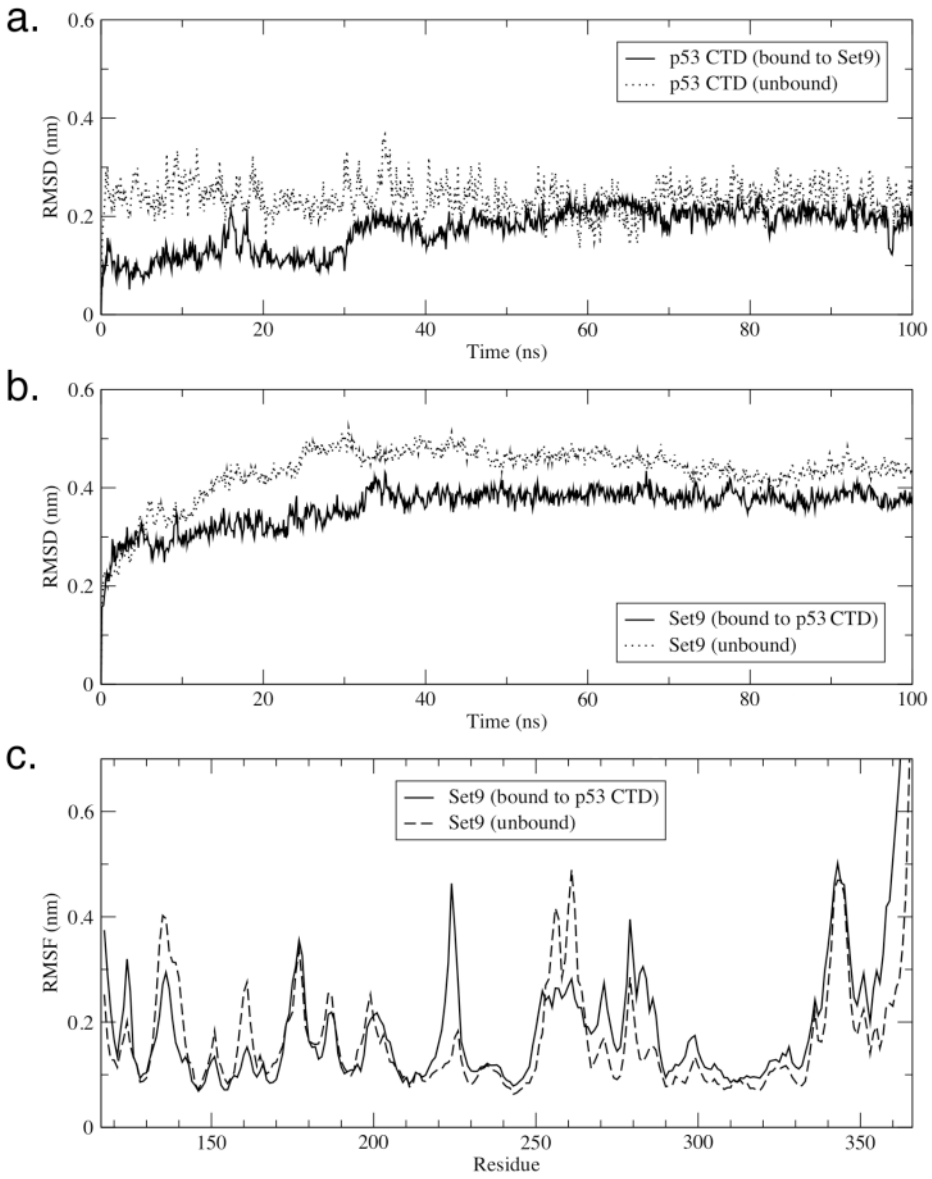

Figure S15. RMSD and RMSF analysis for 1XQH. Panel **(a)** shows the average backbone RMSD for the three replicates of the p53 CTD in complex with Set9 (solid line), and in the absence of Set9 (dotted line). Panel **(b)** shows the average backbone RMSD for the three replicates of the Set9 receptor in complex with the p53 CTD (solid line) and in the absence of the p53 CTD (dotted line). Panel **(c)** represents the RMSF of Set9 in complex with the p53 CTD (solid line), and in the absence of the p53 CTD (dashed line).

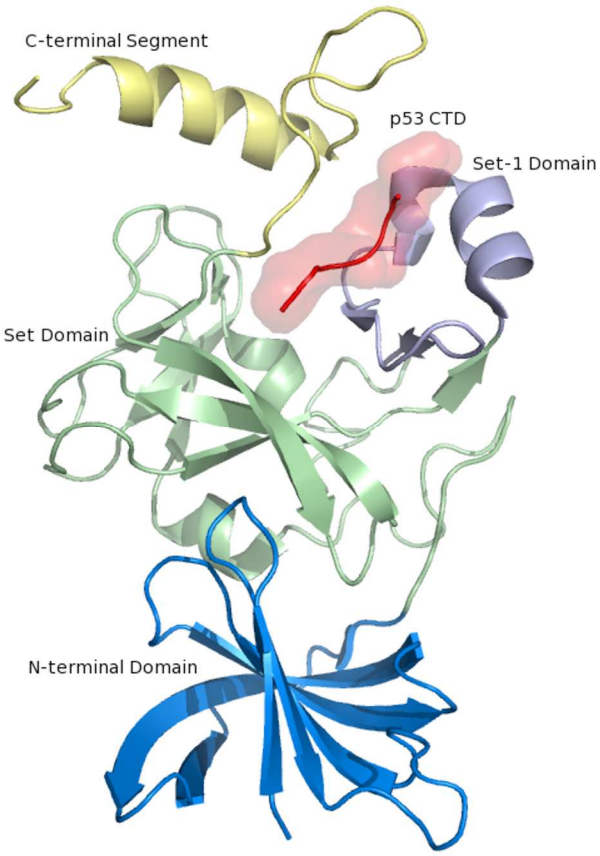

Figure S16. Surface rendering and cartoon of the p53 CTD backbone (shown in red). The receptor Set9 is shown in cartoon, highlighting the N-terminal domain (blue), the Set domain (green), the Set-I domain (purple), and the C-terminal segment (yellow).

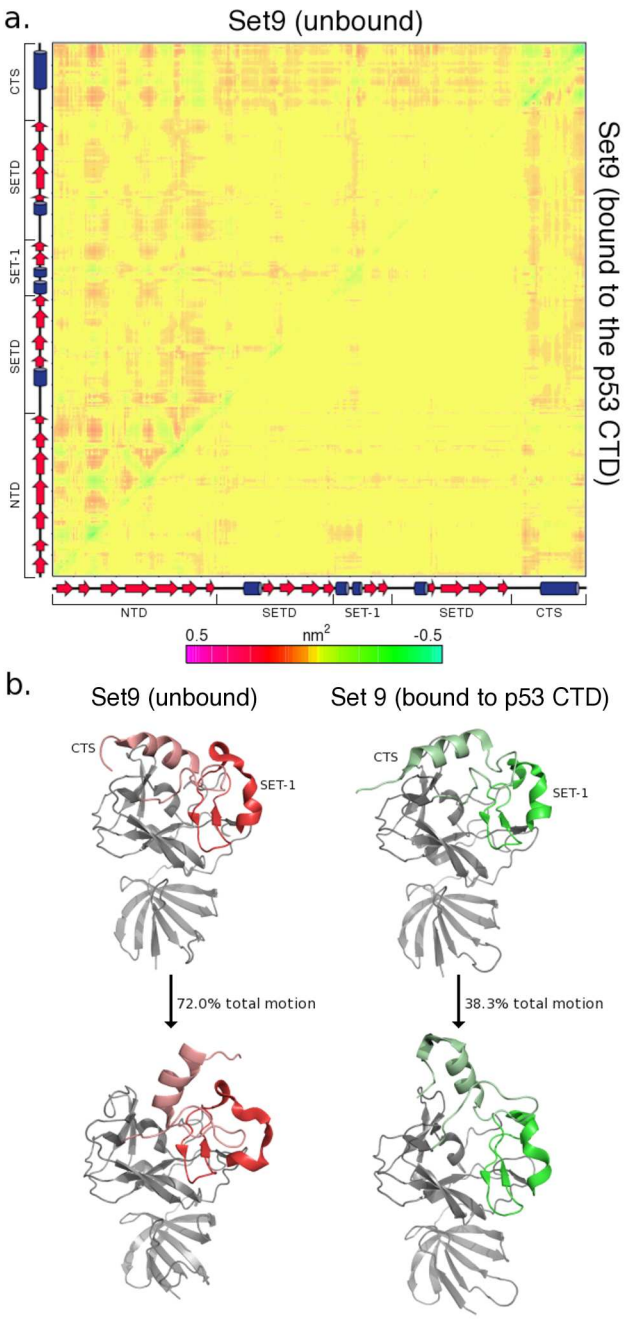

Figure S17. PC analysis for 1XQH. Panel **(a)** shows a covariance matrix illustrating correlated and anti-correlated motions within Set9 in the absence of the p53 CTD (top left) and when bound to the p53 CTD (bottom right). The secondary structure of the Set9 backbone is represented along the axes (from left-to-right, and from bottom-to-top). Panel **(b)** shows the motion of the largest eigenvector on the Set9

structure in the absence of the p53 CTD (left) and when bound to the p53 CTD (right). The sites on Set9 that bind the p53 CTD are colored red and green.

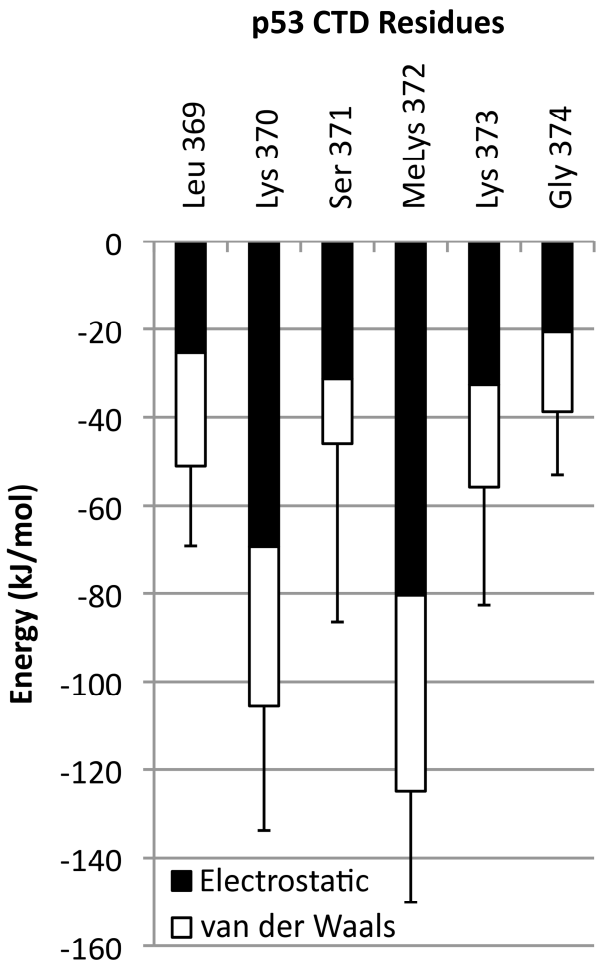

Figure S18. Potential energy of interaction between the p53 CTD and Set9 by residue. The electrostatic contribution is shown in black, and the van der Waals contribution is shown in white. Error bars represent the standard deviation in the sum of the interactions.

Supplemental Tables for Energy Contributions

Table S6. Energy contributions for the interaction between the p53 CTD and S100B(ββ)**.**

Values are in kJ mol^{-1}.

	Electrostatic	van der Waals	Sum
Ser 367	-9.78±21.96	-4.29±7.38	-14.07±23.17
His 368	-38.21±39.42	-14.69±11.56	-52.90±41.08
Leu 369	-1.83±4.60	-14.66±8.45	-16.49±9.63
Lys 370	-16.35±19.15	-4.29±6.66	-20.64±20.27
Ser 371	-23.16±31.55	-0.59±7.67	-23.75±32.47
Lys 372	-7.95±12.81	-0.98±3.14	-8.93±13.19
Lys 373	-5.62±10.98	-7.99±7.90	-13.61±13.52
Gly 374	-0.53±2.21	-2.77±3.47	-3.30±4.12
Gln 375	-24.42±27.74	-7.17±8.52	-31.58±29.02
Ser 376	-3.59±10.73	-1.89±3.05	-5.47±11.15
Thr 377	-20.51±25.64	-2.60±7.01	-23.11±26.58
Ser 378	-43.67±30.46	-6.12±8.90	-49.79±31.73
Arg 379	-45.94±26.77	-24.62±15.15	-70.56±30.76
His 380	-25.57±30.97	-4.63±7.29	-30.20±31.81
Lys 381	-38.71±30.01	-10.66±12.03	-49.37±32.33
Lys 382	-56.82±19.95	-26.29±11.21	-83.11±22.88
Leu 383	-10.75±15.31	-27.56±5.52	-38.31±16.27
Met 384	-10.74±15.39	-9.10±5.70	-19.84±16.41
Phe 385	-0.80±2.58	-7.01±7.49	-7.81±7.92
Lys 386	-25.20±22.44	-20.60±8.02	-45.80±23.83
Thr 387	-18.38±27.80	-13.09±9.65	-31.47±29.43
Glu 389	-18.64±20.40	-7.01±6.36	-25.65±21.37

Table S7. Energy contributions for the interaction between the p53 CTD and Sir2 (PDB:1MA3)**.** Values are in kJ mol^{-1}.

	Electrostatic	van der Waals	Sum
Arg 379	-3.31±6.53	-15.32±8.05	-18.63±10.36
His 380	-28.64±14.60	-18.51±7.65	-47.15±16.49
Lys 381	-1.98±4.97	-23.63±3.52	-25.60±6.09
AcLys 382	-60.22±13.35	-79.73±10.26	-139.95±16.84
Leu 383	-25.40±9.28	-21.07±5.39	-46.47±10.73
Met 384	-11.65±12.56	-37.76±7.54	-49.42±14.65
Phe 385	-13.43±5.97	-18.65±5.10	-32.08±7.85
Lys 386	-22.37±25.19	-6.49±9.22	-28.86±26.82
Thr 387	-9.18±16.17	-8.88±7.47	-18.06±17.81

Table S8. Energy contributions for the interaction between the p53 CTD and cyclin A (PDB:1H26)**.** Values are in kJ mol^{-1}.

	Electrostatic	van der Waals	Sum
Ser 378	-49.03±24.72	-5.08±10.30	-54.11±26.78
Arg 379	-45.77±22.86	-29.49±8.49	-75.26±24.38
His 380	-85.52±15.74	-7.93±9.21	-93.45±18.23
Lys 381	-58.98±35.09	-12.51±11.14	-71.49±36.81
Lys 382	-11.55±15.98	-11.44±6.90	-22.99±17.41
Leu 383	-5.34±7.83	-27.39±6.98	-32.73±10.49
Met 384	-0.23±1.52	-6.42±4.72	-6.65±4.96
Phe 385	-4.45±7.13	-37.06±9.13	-41.51±11.58
Lys 386	-7.40±10.35	-10.78±7.95	-18.19±13.05

Table S9. Energy contributions for the interaction between the p53 CTD and the CBP bromodomain (PDB:1JSP)**.** Values are in kJ mol^{-1}.

	Electrostatic	van der Waals	Sum
Ser 367	-20.75±20.13	-10.40±7.34	-31.15±21.43
His 368	-72.96±23.12	-10.23±12.71	-83.19±26.38
Leu 369	-5.80±9.80	-13.87±6.97	-19.67±12.02
Lys 370	-9.65±13.95	-11.88±6.23	-21.54±15.27
Ser 371	-30.40±33.74	-4.80±7.61	-35.20±34.58
Lys 372	-8.85±16.22	-12.44±7.89	-21.29±18.04
Lys 373	-37.89±32.07	-23.95±18.23	-61.85±36.89
Gly 374	-7.77±8.50	-10.55±7.91	-18.32±11.61
Gln 375	-16.09±16.83	-15.67±9.29	-31.76±19.23
Ser 376	-3.22±8.73	-8.19±5.43	-11.41±10.28
Thr 377	-0.13±1.85	-3.11±3.47	-3.24±3.93
Ser 378	-8.82±16.53	-3.13±6.27	-11.95±17.67
Arg 379	-12.61±15.67	-9.23±7.80	-21.84±17.50
His 380	-50.79±30.06	-2.52±16.68	-53.32±34.38
Lys 381	-0.04±1.02	-5.35±5.31	-5.39±5.41
AcLys 382	-12.44±15.22	-32.12±23.78	-44.57±28.23
Leu 383	-1.26±1.57	-31.32±10.54	-32.57±10.66
Met 384	-16.39±10.90	-18.67±5.96	-35.06±12.42
Phe 385	-22.34±11.56	-40.41±13.87	-62.76±18.06
Lys 386	-8.06±12.78	-18.39±6.94	-26.46±14.54

Table S10. Energy contributions for the interaction between the p53 CTD and the Set9 (PDB:1XQH)**.** Values are in kJ mol^{-1}.

	Electrostatic	van der Waals	Sum
Leu 369	-25.20±12.95	-25.83±12.71	-51.03±18.15
Lys 370	-69.35±25.97	-36.23±11.15	-105.58±28.26
Ser 371	-31.21±38.94	-14.70±11.70	-45.91±40.66
MeLys 372	-80.42±21.17	-44.42±14.03	-124.85±25.40
Lys 373	-32.52±24.56	-23.10±11.21	-55.62±27.00
Gly 374	-20.65±12.60	-18.12±6.51	-38.77±14.18